

Mid-Holocene East Asian summer climate as simulated by the PMIP2 models

Wang Tao^{a,b,c,*}, Wang Huijun^{a,b}, Jiang Dabang^{a,b}

^a Nansen-Zhu International Research Centre, Institute of Atmospheric Physics, Chinese Academy of Sciences, Beijing, China

^b Climate Change Research Center, Chinese Academy of Sciences, Beijing, China

^c Graduate University of Chinese Academy of Sciences, Beijing, China

ARTICLE INFO

Article history:

Received 15 July 2009

Received in revised form 19 January 2010

Accepted 24 January 2010

Available online 1 February 2010

Keywords:

Mid-Holocene

Model

Data-model comparison

East Asia

ABSTRACT

In the present study, datasets derived from twelve coupled ocean–atmosphere general circulation models (OAGCMs) in the Paleoclimate Modelling Intercomparison Project phase two were used to analyze the East Asian summer climate during the mid-Holocene (about 6000 calendar years ago). On the whole, the OAGCMs reproduced warmer and wetter summer climate conditions in East Asia during the mid-Holocene. The multi-model ensemble showed that in East Asia, the regionally-averaged summer surface air temperature (SAT) increased by 0.89 °C, summer precipitation was 5.8% higher, and an obviously strengthened southerly wind corresponded to a strong summer monsoon in the mid-Holocene when compared to preindustrial levels. The data-model comparison in China reveals a good agreement between the OAGCMs' results and the reconstructed changes in the summer SAT in East China during the mid-Holocene. In North China, the simulated SAT anomalies are 0.5 °C lower overall than reconstruction. In contrast, the OAGCMs fail to capture the strongest warming in the southern Qinghai–Tibetan Plateau. On the other hand, the simulated precipitation agrees well with proxy data except for in the central parts of China, where the simulated summer precipitation disagrees in sign with reconstruction. In addition, there is a large spread among the simulations, particularly over and around the Qinghai–Tibetan Plateau, and inter-model discrepancies are larger for precipitation than for SAT as a whole.

Crown Copyright © 2010 Published by Elsevier B.V. All rights reserved.

1. Introduction

Paleoclimate modelling is important for the evaluation and development of climate models. These simulations also can be used to explore potential dynamic mechanisms responsible for past climate changes over a range of time scales (Jansen et al., 2007). For the Paleoclimate Modelling Intercomparison Project (PMIP) (Joussaume and Taylor, 1995), the mid-Holocene (MH, about 6000 calendar years ago) is one of the periods of concern.

The MH is well known as a warm climate interval when the Northern Hemisphere received more insolation in the summer but less in the winter compared to the present level (Berger, 1978). Given that the MH climate conditions were greatly different than those of today and that the availability of a variety of proxy data covering this warm period provides an opportunity to evaluate model results, numerous simulations, particularly those participating in phase one of the PMIP (PMIP1), were performed to address the MH climate using atmospheric general circulation models (AGCMs) and AGCMs coupled with a slab ocean model (e.g., Kutzbach and Guetter, 1986; Mitchell

et al., 1988; Wang, 1992; Kutzbach and Liu, 1997; Masson and Joussaume, 1997; Wang, 1999). The general finding of these studies is that the MH Earth's orbital forcing alone could have strengthened substantially the African and Asian monsoons. However, these simulations still cannot fully explain vegetation and hydrological changes suggested by proxy data in the Afro-Asian monsoon areas (e.g., Yu and Harrison, 1996; Harrison et al., 1998; Joussaume et al., 1999; Masson et al., 1999; Braconnot et al., 2002; Chen et al., 2002; Coe and Harrison, 2002; Bonfils et al., 2004).

Up until now, numerous studies have addressed ocean feedback (e.g., Braconnot et al., 1999, 2000; Zhao et al., 2005, 2007a; Ohgaito and Abe-Ouchi, 2009) and the large-scale features of atmospheric general circulation (e.g., Gladstone et al., 2005; Braconnot et al., 2007b) during the MH, particularly under the framework of the second phase of the PMIP (PMIP2; Harrison et al., 2002; Braconnot et al., 2003; Crucifix et al., 2005), in which twelve OAGCMs were used to simulate the MH climate. In recent years, data-model comparisons have also been performed in Europe and Africa (e.g., Peyron et al., 2006; Brewer et al., 2007; Wohlfahrt et al., 2008). On the whole, the PMIP2 OAGCMs' simulations were in better agreement with proxy data than the PMIP1 simulations due to the addition of an interactive ocean component into climate models (Braconnot et al., 2007a).

A wealth of proxy data have revealed that the Holocene megathermal period occurred 8.5–3.0 ka before present (BP) and reached a maximum during 7.2–6.0 ka BP in China when a strong summer

* Corresponding author. Nansen-Zhu International Research Centre, Institute of Atmospheric Physics, Chinese Academy of Sciences, Beijing, China. Fax: +86 10 82995057.

E-mail address: wangtao@mail.iap.ac.cn (W. Tao).

Table 1
Twelve OAGCMs within the PMIP2.

Models	Horizontal resolution	Flux adjustments	References
CCSM	T85	No	Otto-Bliesner et al. (2006)
CSIRO-Mk3L-1.0	R21	Yes	Phipps (2006)
CSIRO-Mk3L-1.1	R21	Yes	Phipps (2006)
ECHAM5-MPIOM1	T63	No	Roeckner et al. (2003)
FGOALS-1.0g	5×4°	No	Yu et al. (2004)
FOAM	R15	No	Jacob et al. (2001)
GISSmodelE	5×4°	No	Schmidt et al. (2006)
IPSL-CM4-V1-MR	3.75×2.5°	No	Martí et al. (2005)
MIROC3.2	T42	No	K-1 model developers (2004)
MRI-CGCM2.3.4fa	T42	Yes	Yukimoto et al. (2006)
MRI-CGCM2.3.4nfa	T42	No	Yukimoto et al. (2006)
UBRIS-HadCM3M2	3.75×2.5°	No	Gordon et al. (2000)

monsoon prevailed over the East Asian monsoon area. The data also showed that the surface temperature was 1–4 °C higher and precipitation was 40–100% greater than the present values in China (e.g., Kong et al., 1990; An et al., 1991; Yao et al., 1991; Shi et al., 1992). The recent studies using the PMIP2 OAGCMs' results inspire us to ask these questions: what summer climate changes occurred in the East Asian monsoon area in the MH according to these OAGCMs' simulations, and to what extent proxy data and the models' results are compatible in

mainland China where proxy data are plentiful. Because these issues remain unclear, here we made use of a suite of twelve OAGCMs' simulations within the PMIP2 to examine the MH climate in East Asia and then to perform a data-model comparison in China. It should be noted that as a first step in exploring the MH climate in East Asia, the summer (June, July, and August) climate was investigated in the present study because the strongest regional climate changes in climate model experiments occurred in this season in the MH (e.g., Wang, 2000, 2002).

This paper is organized as follows: Section 2 describes the boundary conditions and experimental design and introduces the PMIP2 models; Section 3 compares the current climate status derived from the twelve OAGCMs with observation; in Section 4, the outputs from the OAGCMs are used to analyze the MH summer climate changes in East Asia and then compared to proxy data and with each other; finally, Section 5 presents the conclusions of this study.

2. Models, boundary conditions, and experimental design

In the PMIP2, the MH experiments were forced by an eccentricity of 0.018682, an obliquity of 24.105°, a precession of 0.87° (Berger, 1978), and an atmospheric CH₄ concentration of 650 ppbv. On the other hand, the control experiments, i.e., the preindustrial (PI) climate simulations, were forced by an eccentricity of 0.016724, an obliquity of 23.446°, a precession of 102.04°, and an atmospheric CH₄

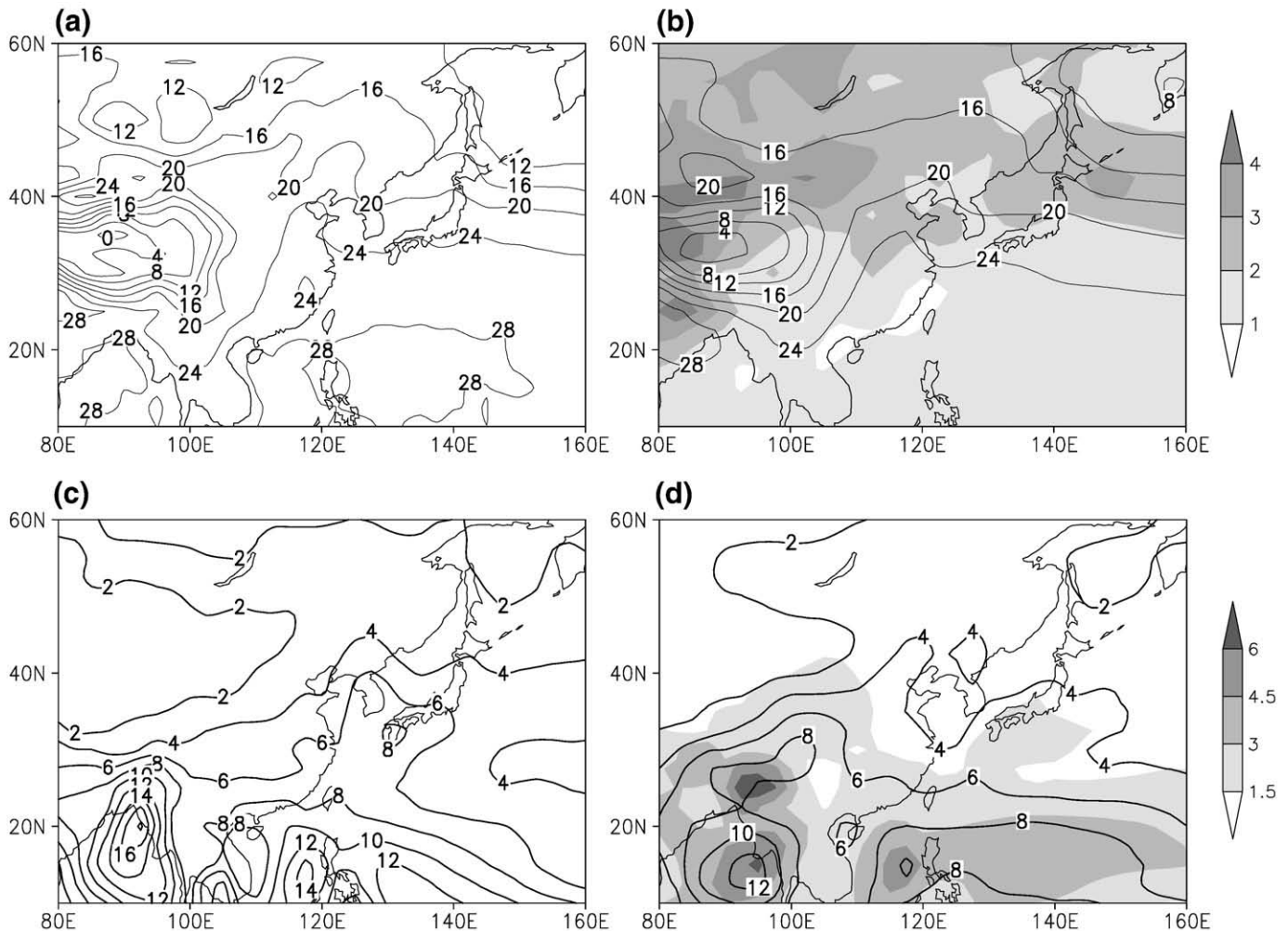


Fig. 1. Surface air temperature (top) and precipitation (bottom) in summer: (a) climatology for the period of 1970–1999 from the NCEP/NCAR reanalysis data (unit: °C); (b) twelve-OAGCM ensemble mean simulation for the PI, in which the shaded area stands for the standard deviation of the simulated SAT by the twelve OAGCMs (unit: °C); (c) climatology for the period of 1979–2006 from the CMAP (unit: mm d⁻¹); (d) same as (b), but for precipitation (unit: mm d⁻¹).

concentration of 760 ppbv. The atmospheric CO₂ concentration was held at 280 ppmv for both periods. Other boundary conditions, such as vegetation, ice sheets, topography, coastlines, greenhouse gases except for atmospheric CH₄ concentration, solar constant, and initial ocean state were kept the same for both the PI and MH simulation.

Twelve OAGCMs (see Table 1) were used in the MH experiments in the framework of the PMIP2. In this study, the outputs of the last 50 years derived from each OAGCM were analyzed. The statistical significance was assessed by applying a Student's *t*-test to the differences between the PI and the MH simulations. In addition, the NCEP/NCAR monthly reanalysis data for the period 1970–1999 (Kalnay et al., 1996) and the CMAP precipitation data for the period 1979–2006 (Xie and Arkin, 1997) were used to evaluate the fidelity of the control simulations for the present climatology.

3. Evaluation of the models' climatology

It is important to examine whether OAGCMs can reliably reproduce East Asian summer climatology because this ability is directly related to the utility of these models for investigating the MH climate changes in this region. Fig. 1 illustrates that the multi-model ensemble mean of summer surface air temperature (SAT) and precipitation agrees well with observations on a large scale. For the simulated SAT

(Fig. 1b), the spatial correlation coefficient is high, up to 0.97 with respect to the NCEP/NCAR reanalysis data. However, there is a large amount of cooling bias in mainland China and the western Pacific Ocean. The maximum standard deviation of the simulated SAT appears in western China and eastern India, implying a large discrepancy for the SAT among OAGCMs' simulations in these two regions. The observational summer precipitation climatology from 1979 to 2006 is shown in Fig. 1c. More precipitation is centralized in the tropics, and precipitation gradually decreases at higher latitudes. The multi-model ensemble mean of summer precipitation for the PI is in good agreement with the observations as a whole (Fig. 1d), and the spatial correlation coefficient between them is 0.89. Nevertheless, the OAGCMs underestimate precipitation in the low latitudes of East Asia and in the Bay of Bengal. Moreover, a large discrepancy for the OAGCM simulated precipitation also appears over and around these regions.

Fig. 2 shows the ensemble mean of the summer wind at 850 hPa in East Asia. The spatial patterns of the wind field are very consistent between the multi-model ensemble mean for the PI and the NCEP/NCAR reanalysis data from 1970 to 1999. Observational southerly winds over South China and an anticyclonic circulation over the western Pacific are well captured by the multi-model ensemble mean. Nevertheless, differences between observational data and the simulation still exist. For instance, there is an anomalous cyclone over the

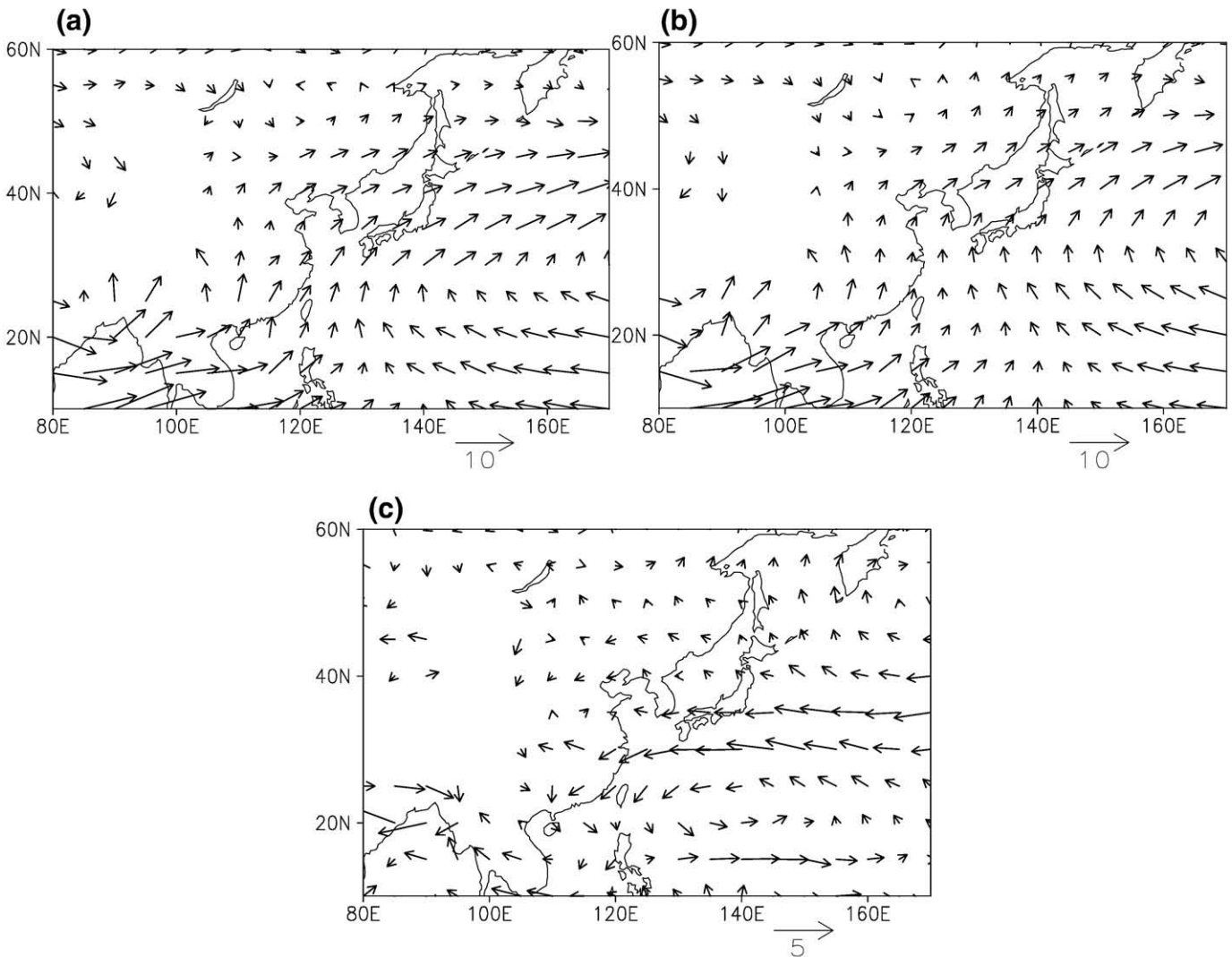


Fig. 2. Summer wind field at 850 hPa (unit: m s⁻¹): (a) climatology for the period of 1970–1999 from the NCEP/NCAR reanalysis data; (b) twelve-OAGCM ensemble mean simulation for the PI; (c) simulation minus observation. Regions with elevations higher than 1500 m are blank over the Qinghai–Tibetan Plateau.

western Pacific and a subtropical easterly wind around 40°N in the simulation (Fig. 2c) indicating a weak western Pacific subtropical high and an associated weak East Asian summer monsoon circulation over South China in the OAGCMs. This underestimation of the circulation intensity is consistent with the OAGCM simulated weak precipitation over the East Asian region mentioned before.

To assess quantitatively the reproducibility of the OAGCMs' simulations for East Asian summer climatology within the region of 10–60°N and 80–160°E, the values of three statistical variables were calculated. There are the regionally-averaged summer SAT and precipitation, the simulation error of regionally-averaged summer SAT and precipitation, and the spatial correlation coefficient between simulation and observation for each climate variable. As shown in Table 2, cold biases are present in most models and in the multi-model ensemble mean. It should be noted that within the PMIP2 PI simulations, atmospheric CO₂, CH₄, and N₂O concentrations remained at 280 ppmv, 760 ppbv, and 270 ppbv, respectively, which are lower than the average values of 344 ppmv, 1591 ppbv, and 305 ppbv for the period of 1970–1999. These differences in greenhouse gases' forcings can explain about 0.6 °C of the cold biases between the PI simulations and the reanalysis data (Folland et al., 2001; Trenberth et al., 2007). In contrast, ECHAM5-MPIOM1, GISSmodelE, and MIROC3.2 show warming errors in the regionally-averaged summer SAT. In addition, the standard deviation of SAT is 1.3 °C among the models. The spatial correlation coefficients between OAGCMs' SAT and observation are all higher than 0.90, indicating that the geographical distribution of summer SAT in East Asia is well simulated by these models. In particular, the multi-model ensemble mean has the highest spatial correlation coefficient, as high as 0.97. On the other hand, the multi-model ensemble mean of regionally-averaged summer precipitation is 4.71 mm d⁻¹, which is underestimated by 5.2% compared to the observational value of 4.97 mm d⁻¹. The spatial correlation coefficient for the multi-model ensemble mean reaches 0.89, which is higher than any of the individual model results. Among the models, the standard deviation is 0.69 mm d⁻¹, which accounts for 13.9% of the observational value (4.97 mm d⁻¹). Overall, the OAGCMs' ability to reproduce summer precipitation climatology is poor relative to their ability to reproduce SAT in East Asia.

Taken together, the multi-model ensemble mean of the OAGCMs reproduces observational values and patterns of summer SAT and precipitation in East Asia quite well. Comparatively, it gives a better performance than any individual model. In general, it offers realistic

representations of the state of the current summer climate in East Asia. Therefore, using the multi-model ensemble mean to investigate the MH summer climate in East Asia appears to be a reliable approach.

4. The simulated MH summer climate

4.1. Surface air temperature, precipitation, and monsoon

Changes in the MH Earth's orbital parameters led to about 5% larger incoming solar radiation in the northern extra-tropical latitudes in the summer (Berger, 1978), which gave rise to different MH summer climate conditions from the PI period. As shown in Fig. 3a, SAT increased over the landmass within 30–60°N and over the western North Pacific within 40–60°N. The warming maximums were located in Xinjiang province of China and east of the Lake Baikal. In addition, the magnitude of terrestrial surface warming was generally larger compared to the warming over the ocean at similar latitudes.

In the MH, the amount of summer precipitation was enhanced in most regions of the East Asian landmass (Fig. 3b). Notable changes were registered at 20–40°N. The maximum positive anomalies for precipitation were located in the southern Qinghai–Tibetan Plateau and eastern India, where precipitation increased by more than 80%.

Table 2

The values of statistical variables for summer SAT and precipitation in East Asia (10°–60°N, 80°–160°E). RAT and RAP denote regionally-average summer SAT and precipitation; RAET denotes the simulation error of regionally-averaged summer SAT; RAEP denotes the simulation error ratio of regionally-averaged summer precipitation relative to observation; SCC denotes the spatial correlation coefficient between simulation and observation; STD denotes the standard deviation of the twelve OAGCMs' results.

Model	RAT (°C)	RAET (°C)	SCC for SAT	RAP (mm d ⁻¹)	RAEP (%)	SCC for precipitation
<i>Observational RAT equals 20.3 °C, and RAP equals 4.97 mm d⁻¹</i>						
CCSM	18.1	-2.2	0.94	4.26	-14.4	0.83
CSIRO-Mk3L-1.0	19.6	-0.7	0.94	5.54	11.5	0.78
CSIRO-Mk3L-1.1	20.3	0.0	0.94	5.67	14.1	0.81
ECHAM5-MPIOM1	21.3	1.0	0.93	5.41	8.8	0.82
FGOALS-1.0g	20.2	-0.1	0.91	3.42	-31.2	0.25
FOAM	17.5	-2.8	0.90	4.92	-0.9	0.35
GISSmodelE	20.5	0.2	0.90	4.28	-13.8	0.65
IPSL-CM4-V1-MR	18.3	-2.0	0.93	3.96	-20.2	0.77
MIROC3.2	20.8	0.5	0.95	4.73	-4.7	0.74
MRI-CGCM2.3.4fa	19.0	-1.3	0.96	5.05	1.7	0.81
MRI-CGCM2.3.4nfa	17.4	-2.9	0.96	4.03	-19.0	0.79
UBRIS-HadCM3M2	20.2	-0.1	0.95	5.26	5.8	0.87
Ensemble mean	19.4	-0.9	0.97	4.71	-5.2	0.89
Inter-model STD	1.3			0.69	13.9	

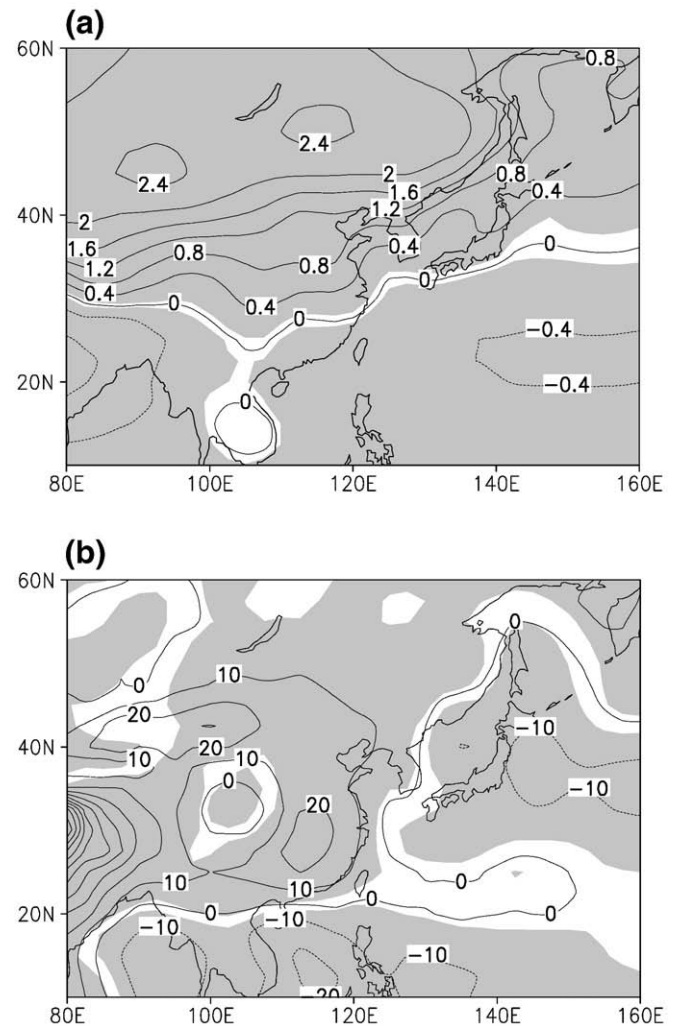


Fig. 3. (a) Twelve-OAGCM simulated ensemble mean differences (MH minus PI) in summer SAT (unit: °C); (b) twelve-OAGCM simulated ensemble mean fractional ratio of summer precipitation changes in the MH relative to the PI. Areas with confidence levels exceeding 95% are shaded.

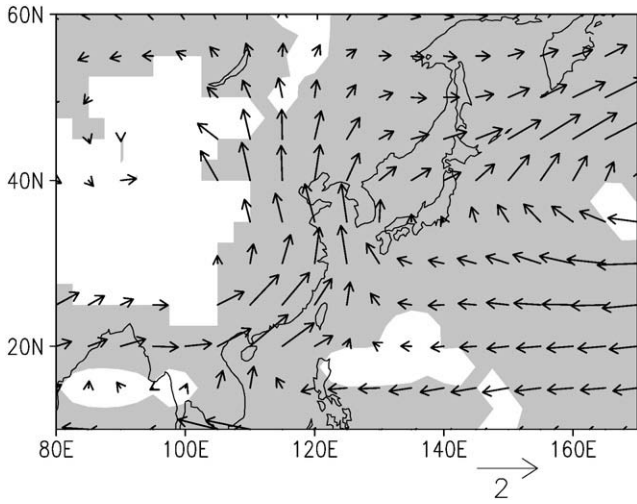


Fig. 4. Twelve-OAGCM simulated ensemble mean differences (MH minus PI) in summer wind field at 850 hPa (unit: $m s^{-1}$). Areas with confidence levels exceeding 95% are shaded, and the regions with elevations higher than 1500 m are blank over the Qinghai–Tibetan Plateau.

The other two large positive anomalies appeared in South China and the Xinjiang province, which implied the existence of wetter climate conditions in the middle and lower reaches of the Yangtze River valley and in the Xinjiang area. On the contrary, summer precipitation decreased over the western North Pacific.

During the MH summer, obvious southerly wind anomalies were present over East Asia (Fig. 4), corresponding to a strong summer monsoon (Tao and Chen, 1987). Additionally, there was an anomalous anticyclone over the Northwest Pacific, which could be related to the strengthening and northward migration of the western North Pacific subtropical high. In general, a combination of these two anomalies in the wind field at 850 hPa allowed for increased water vapor transport from the South China Sea to the East Asian continent, which was the main cause for the increase of precipitation throughout the area of eastern China in the MH, particularly in South China (e.g., Zhao et al., 2007b).

4.2. Data-model comparison

According to a summary of the environmental evolution of China over the last 20 ka (An et al., 1990), Shi et al. (1993) described climatic and environmental features in the MH. In addition to these records, we also refer to a wealth of recent proxy data in China (see Table 3). The overview scenario of the MH SAT changes in mainland China is illustrated in Fig. 5a. On the whole, it can be estimated that the MH annual SAT was 2–3 °C higher in East China and 3–4 °C higher in West China and northeastern China than at present. Interestingly, there are three records that depict colder conditions. Two of them are located in Inner Mongolia, and the third is located in the western Qinghai–Tibetan Plateau. These imply uncertainties embedded in the proxy data.

The shaded area in Fig. 5a shows that the twelve-OAGCM ensemble mean predicts warmer summer climate conditions in China in the MH. The SAT is increased by 0.5–3.0 °C from about 25°N northward. The geographical distribution of the simulated summer SAT anomalies is nearly parallel to the reconstructed annual one in most parts of East China, but the values are systemically lower. Since the MH summer surface warming is somewhat weaker than the annual mean suggested by Shi et al. (1993), the OAGCMs are therefore consistent with the reconstructed changes of the MH summer SAT in East China. In North China, the simulated SAT increased by 2.5–3.0 °C. These values are about 0.5 °C lower than the reconstruction. In contrast, the OAGCMs fail to reproduce the strongest warming in the southern Qinghai–Tibetan Plateau, where the reconstructed SAT increased by more than 5 °C.

Precipitation is another important indicator for environmental conditions, which has a direct impact on regional effective humidity. Logically, the reconstructed changes in regional effective humidity should partly reflect the direction of the precipitation change. Therefore, the MH precipitation and environmental changes are summarized here in terms of the reconstructed records (Fig. 5b). Restricted by the temporal resolution of these proxy data, the reconstructed changes are valid only for an annual situation. However, it is still suitable to use the reconstructed annual precipitation changes to perform a data-model comparison for summer because about 40–60% of annual precipitation occurs during the summer over most parts of China (Fu et al., 1992). According to the reconstruction, the MH precipitation in China was more plentiful than at present. For example,

Table 3
Proxy data in China in the MH.

Sites	Sample type	Lat. (°N)	Long. (°E)	Reconstructed environment (compared to the present)	References
Baahar Nuur Lake	Lake core	39.3	109.3	Higher summer SAT and more humid condition	Guo et al. (2007)
Barkol Lake	Lake core	43.5	92.8	Warmer and wetter condition	Xue and Zhong (2008)
Bayanchagan Lake	Lake core	41.7	115.2	No change or a little drier	(Jiang et al., 2006; Jiang and Liu, 2007)
Bosten Lake	Lake core	41.9	86.7	Warmer and moister condition	Wünnemann et al. (2003)
Dadiwan Profile	Fluvial profile	35	105.9	Distinct humid and warm	(An et al., 2003; Tang and An, 2007)
Daihai Lake	Lake core	40.5	112.6	More humid; annual precipitation 40% higher	(Wang and Feng, 1992; Sun et al., 2006)
Dajiuhe Section	Peat core	31.5	110	Best condition of water and heat	Zhu et al. (2006)
Diaoqiao Lake	Lake core	41.3	112.4	Annual precipitation 20–50% higher and annual SAT 3–6 °C warmer	Shi and Song (2003)
Dongge Cave	Stalagmite	25.3	108.1	Higher annual precipitation	Wang et al. (2005)
Guliya	Ice core	35.3	81.5	Colder and drier condition	Thompson et al. (1997)
Hidden Lake	Lake core	29.8	92.5	Annual precipitation 30% higher and annual SAT 2–3 °C warmer	Tang et al. (2000)
Hongshui River	Lake core	38.2	102.8	Warmer and annual precipitation higher	Zhang et al. (2000)
Hoton-Nur	Lake core	48.6	88.3	Annual precipitation 50–60% higher	Rudaya et al. (2009)
Huguangyan Maar Lake	Lake core	21.2	110.3	Warmer and wetter	Wang et al. (2007)
Juyanze Lake	Lake core	41.9	101.5	Colder and drier condition	Chen et al. (2003a)
Qinghai Lake	Lake core	36.5	100	Warmer and annual precipitation 70–80% higher	(Wang and Feng, 1992; Liu et al., 2002; Shen et al., 2005)
Ren Co Lake	Lake core	30.7	96.7	Annual precipitation 30% higher and annual SAT 2–3 °C warmer	Tang et al. (2000)
Sujiawan Profile	Fluvial profile	35.5	104.5	Distinct humid and warm	(An et al., 2003; Tang and An, 2007)
Sumxi Co	Lake core	34	81	Warmer and wetter	Gasse et al. (1991)
Toudaohu Lake	Lake core	38.4	105.1	Colder and drier condition	Chen et al. (2003a)
Wulungu Lake	Lake core	47.2	87.2	Warmer and wetter condition	Jiang et al. (2007)
Yanhaizi Lake	Lake core	40.1	108.4	Warmer and drier condition	Chen et al. (2003b)
Yiema Lake	Lake core	39.1	103.7	Much moister than present	Chen et al. (1999)
Zige Tangco	Lake core	32.1	90.8	Warmer and wetter condition	Wu et al. (2007)

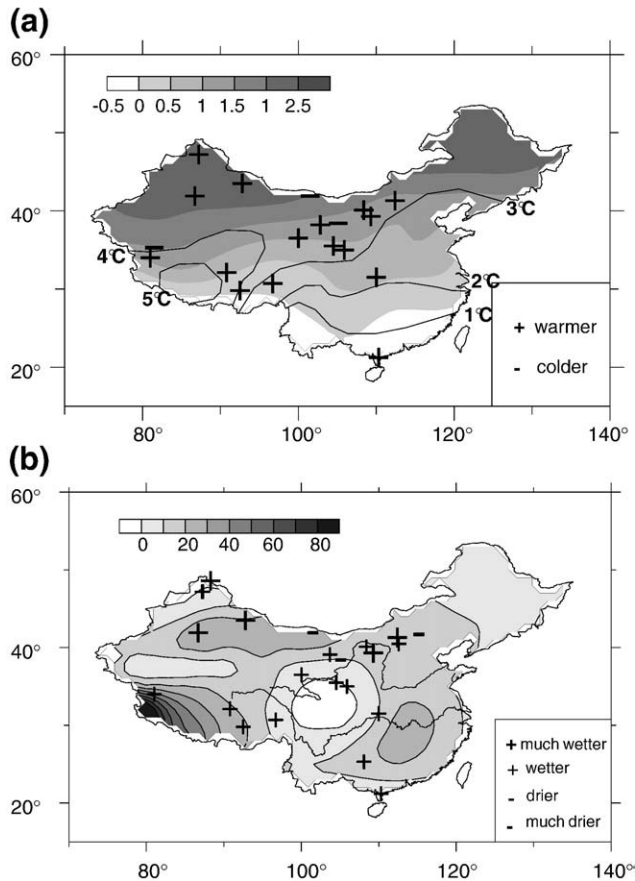


Fig. 5. (a) The reconstructed MH SAT changes with reference to the present in China on the basis of proxy data listed in Table 3. The contours are modified from Shi et al. (1993), and the shaded area stands for twelve-OAGCM simulated ensemble mean differences in summer SAT between the MH and the PI (unit: °C). (b) Plus or minus sign is the same as in (a), but for annual humidity or precipitation. The contours denote twelve-OAGCM simulated ensemble mean fractional ratio of summer precipitation changes at the MH relative to the PI.

in the Qinghai Lake area, annual precipitation was 70–80% higher than it is today. At Daihai Lake, Hidden Lake, and Ren Co Lake, annual precipitation increased by about 30%.

As seen in Fig. 5b, the OAGCMs' results are consistent with reconstruction in the Ren Co Lake and Hidden Lake areas, where summer precipitation was increased by 10–30%, whereas the OAGCMs underestimate the magnitude of the precipitation change at Qinghai Lake. In the Daihai Lake and Diaojiao Lake areas, simulated precipitation was increased by about 20%, which was also a little lower than proxy data. Overall, the MH summer precipitation as simulated by the OAGCMs was enhanced in most parts of China, especially in South China, the Xinjiang area, and the southern Qinghai–Tibetan Plateau. These results are in good agreement with the proxy data. In contrast, in the center of China there are large differences between the OAGCMs' results and the reconstruction, with less precipitation found in the models while a wetter condition is suggested by proxy data. The model-data comparison therefore shows that the OAGCMs disagree in sign with the reconstructed summer precipitation changes in the central parts of China.

In addition, a model-data comparison was also performed model by model (figures not shown here). It was shown that all OAGCMs simulated the robust warming in North China well. Some models reproduced a weak increase in summer SAT in East China, such as FGOALS-1.0g, ECHAM5-MPIOM1, MIROC3.2, and MRI-CGCM2.3.4nfa. In addition, all OAGCMs, except for IPSL-CM4-V1-MR, failed to reproduce the robust warming in the southern Qinghai–Tibetan Plateau. On the whole, the IPSL-CM4-V1-MR simulated spatial pattern

in summer SAT is the most consistent with proxy data in China. For the MH precipitation changes, most OAGCMs reproduced wetter conditions in East China and the Qinghai–Tibetan Plateau. On the contrary, drier conditions occurred in central parts of China in CCSM, CSIRO-Mk3L-1.0, CSIRO-Mk3L-1.1, ECHAM5-MPIOM1, FGOALS-1.0g, IPSL-CM4-V1-MR, and MIROC3.2, which disagrees with the proxy data. Taken together, UBRIS-HadCM3M2, MRI-CGCM2.3.4fa, and MRI-CGCM2.3.4nfa reproduced better MH precipitation changes in China with reference to the proxy data.

4.3. Inter-model comparison

It is interesting to examine the common and different responses of the twelve OAGCMs to the same MH forcings and then to quantify the range of uncertainty among the models. Within the East Asian monsoon area (20–50°N, 90–130°E), the regional average of summer SAT and precipitation in the PI, regionally-averaged differences in summer SAT between the MH and the PI, the fractional ratio of regionally-averaged summer precipitation changes in the MH relative to the PI, and the standard deviations of regionally-averaged SAT and percentage changes in precipitation during the summer over the 50-year integration period are respectively calculated for each OAGCM and their ensemble mean (see Table 4). As for summer SAT, the twelve-OAGCM ensemble mean regional averages are 19.54 °C and 20.43 °C in the PI and MH, respectively. The regional average difference of SAT is 0.89 °C, ranging across the models from 0.57 °C (ECHAM5-MPIOM1) to 1.21 °C (FOAM) with a standard deviation of 0.24 °C for all of the OAGCMs. It should be emphasized that the standard deviation of regionally-averaged summer SAT is only 0.09 °C for the 50-year multi-model ensemble mean result, which is smaller than that of the individual model, ranging from 0.20 °C to 0.34 °C for each period. The summer SAT of the multi-model ensemble mean consequently has the smallest interannual variability represented by the standard deviation of the regionally-averaged summer SAT over the 50-year period.

The twelve-OAGCM ensemble mean fractional ratio of regionally-averaged summer precipitation changes is 5.8%, suggesting wetter summer climate conditions in the MH. However, it can be seen in Table 4 that there are large discrepancies among the OAGCMs' results. The regional average precipitation in the PI varies from 3.77 mm d⁻¹ (FGOALS-1.0g) to 5.83 mm d⁻¹ (FOAM), with a standard deviation of 0.61 mm d⁻¹ among the OAGCMs. In addition, the fractional ratio of regionally-averaged precipitation changes varies from -0.9% (GISS-modelE) to 14.7% (IPSL-CM4-V1-MR), with a standard deviation of 4.8% among the OAGCMs. As with summer SAT, the smallest interannual variability of summer precipitation is seen in the multi-model ensemble mean. The values are around 1.5%, which are lower than individual model's result, which range from 3.3% to 7.6%.

In addition, inter-model discrepancies for the simulated summer SAT and precipitation differ with region in China. As is well known, a high standard deviation means a large spread in the OAGCMs' responses to the same MH forcings. It can be seen in Fig. 6a that, in general, the large discrepancies in SAT among the OAGCMs are mainly located in the Qinghai–Tibetan Plateau and northeastern China. The maximum standard deviation reaches 1.0 °C in the Qinghai–Tibetan Plateau, which is comparable with the simulated differences of the summer SAT between the MH and PI (Fig. 3a). In northeastern China, the standard deviation is larger than 0.5 °C, which is notably smaller than the simulated summer SAT differences of about 1.5 °C to 2.5 °C. Collectively, there is a large spread in the simulated summer SAT in the Qinghai–Tibetan Plateau. In the rest of Chinese mainland, the standard deviations of the simulated summer SAT by the twelve OAGCMs are much smaller than the twelve-OAGCM simulated ensemble mean changes in summer SAT, which implies robust warming signals.

At present, it is difficult for state-of-the-art OAGCMs to dependably reproduce the distribution and magnitude of summer precipitation in the East Asian monsoon area (e.g., Zhao et al., 1995; Jiang et al., 2005).

Table 4

The values of statistical variables for summer SAT and precipitation in East Asia. RADT denotes regionally-averaged differences of summer SAT between the MH and the PI; RRP denotes the fractional ratio of regionally-averaged summer precipitation changes at the MH relative to the PI; RAT and RAP denote the regional average of summer SAT and precipitation, respectively; STDT denotes the standard deviation of regionally-averaged summer SAT over the 50-year integration period; RSTDP denotes the standard deviation of regionally-averaged percentage changes in summer precipitation over the 50-year integration period; STD denotes the standard deviation of the twelve OAGCMs' result.

Models	Summer SAT				Summer precipitation			
	RADT (°C)	RAT-PI (°C)	STDT-PI (°C)	STDT-MH (°C)	RRP (%)	RAP-PI (mm d ⁻¹)	RSTDP-PI (%)	RSTDP-MH (%)
CCSM	0.80	18.15	0.26	0.32	6.1	4.19	4.6	4.4
CSIRO-Mk3L-1.0	1.17	19.63	0.30	0.30	13.3	4.46	6.3	6.4
CSIRO-Mk3L-1.1	1.20	20.27	0.27	0.30	9.1	4.51	5.3	7.2
ECHAM5-MPIOM1	0.57	21.89	0.34	0.23	4.5	4.85	6.5	5.0
FGOALS-1.0g	0.84	20.38	0.22	0.20	-0.2	3.77	4.1	3.8
FOAM	1.21	17.37	0.34	0.29	3.4	5.83	3.3	4.0
GISSmodelE	0.58	20.49	0.32	0.32	-0.9	5.51	4.6	4.4
IPSL-CM4-V1-MR	1.16	18.16	0.34	0.34	14.7	3.82	5.4	4.4
MIROC3.2	0.70	21.41	0.25	0.27	0.4	5.06	6.1	7.6
MRI-CGCM2.3.4fa	0.83	18.97	0.21	0.25	6.8	4.21	5.5	4.5
MRI-CGCM2.3.4nfa	0.61	17.17	0.23	0.23	3.8	4.23	3.5	3.3
UBRIS-HadCM3M2	0.99	20.65	0.33	0.33	8.0	4.91	5.0	5.8
Ensemble mean	0.89	19.54	0.09	0.09	5.8	4.61	1.6	1.4
Inter-model STD	0.24	1.50			4.8	0.61		

In the IPCC climate projections, there is also a lack of consistency among climate models in terms of Asian precipitation (Christensen et al., 2007). Fig. 6b shows the standard deviation of the simulated fractional ratio of summer precipitation changes in the MH relative to the PI. It can be seen that the discrepancies of the simulated summer

precipitation changes among the twelve OAGCMs are great throughout the Chinese mainland. The maximum standard deviation is situated over western China with a value of up to 60%, while the simulated increases in summer precipitation between the MH and the PI are only around 30% in the Xinjiang area. In East China, the standard deviation is 20%, which is comparable with the simulated summer precipitation changes of 20% to 30% between the MH and the PI. Therefore, the spreads of the simulated summer precipitation changes between the MH and the PI are very different among the OAGCMs in these regions, particularly in the Xinjiang area.

5. Conclusion

The outputs from twelve OAGCMs participating in the PMIP2 were used to investigate several aspects of the simulated summer climate changes in the MH in the East Asian monsoon area, focusing on SAT, precipitation, and monsoons. All OAGCMs predicted warmer conditions in the MH with a regionally-averaged SAT increase of 0.89 °C above the preindustrial value in East Asia (20–50°N, 90–130°E). For precipitation, large discrepancies were displayed in the simulations. Ten models reproduced wetter conditions in East Asia, while FGOALS-1.0g and GISSmodelE reproduced drier conditions in the MH. Moreover, the simulated precipitation was very different across the models. The multi-model ensemble mean fractional ratio of regionally-averaged summer precipitation changes increased by 5.8% in the MH relative to the PI. In the meantime, the OAGCMs' results showed that a stronger MH East Asian summer monsoon was present over the East Asian continent. This strengthened water vapor transport from the South China Sea to the continent, leading to greater moisture conditions in China. The intensified East Asian summer monsoon due to the higher solar radiation in the MH summer, as simulated by the PMIP2 OAGCMs, was consistent with previous simulations (e.g., Wang, 1999; Wei and Wang, 2004) and proxy data (e.g., Neff et al., 2001; Wang et al., 2005) as a whole. Ocean feedback in general amplified climate responses to the MH Earth's orbital forcing in the OAGCMs within the PMIP2 (Braconnot et al., 2007b; Ohgaito and Abe-Ouchi, 2009).

In the MH, most regions of China were believed to have experienced the best water and temperature conditions (Zhu et al., 2006). When comparing the simulations with proxy data, it was found that the twelve-OAGCM ensemble mean reproduced a similar warming pattern to that of a variety of proxy data in China. The simulated differences of summer SAT between the MH and the PI were consistent with reconstructed temperatures in most regions of East

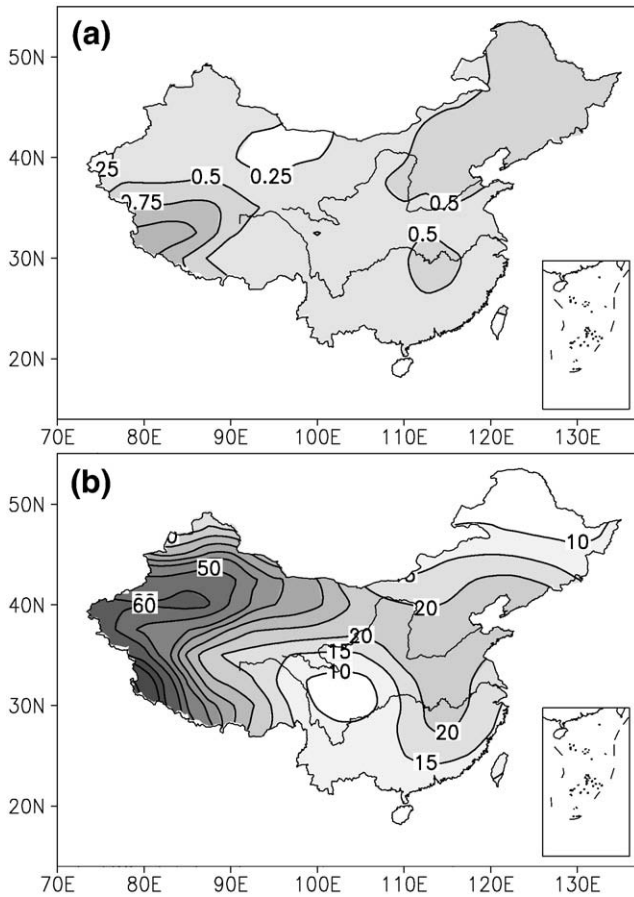


Fig. 6. (a) The standard deviation of the simulated differences (MH minus PI) in summer SAT (unit: °C) by the twelve OAGCMs; (b) the standard deviation of the simulated fractional ratio of summer precipitation changes at the MH relative to the PI by the twelve OAGCMs.

China. In North China, the simulated SAT increased by about 2.5 °C, which was a little lower than the reconstructed level. The spread of the OAGCMs' results was different between northeastern China and the Xinjiang area. Most OAGCMs simulated obvious warming in the Xinjiang area. The high standard deviation indicates large discrepancies among the OAGCMs in northeastern China, and the warming signals are not as robust as those in the Xinjiang area. In the southern Qinghai–Tibetan Plateau, the twelve-OAGCM ensemble mean fails to reproduce a robust warming signal where SAT increases by more than 5 °C as derived from proxy data. In the meantime, the maximum standard deviation is also present for this region. The value of standard deviation is as high as the increase of SAT, implying large discrepancies among the OAGCMs in the southern Qinghai–Tibetan Plateau.

For precipitation, the twelve-OAGCM ensemble mean is in good agreement with reconstructed precipitation and humidity conditions in most parts of China. Nevertheless, there are discrepancies between simulations and proxy data in the central parts of China, where less precipitation in the models disagrees with the wetter conditions suggested by proxy data. Additionally, the OAGCMs reproduced a strong MH precipitation signal in the southern Qinghai–Tibetan Plateau, where it increased by more than 80%.

Inter-model discrepancies for the simulated MH climate differ with region, especially for precipitation. Thus, there are different responses in terms of precipitation to the same MH forcings among the twelve models. These uncertainties of simulated SAT and precipitation should partially account for the above disagreements in the model–data comparison. At the same time, there are many imperfections in the models. For instance, land–ice feedback at high latitudes, water vapor feedback, and a series of other important feedback mechanisms are neglected in the current models. As such, uncertainties both in proxy data and in the OAGCMs (Braconnot and Frankignoul, 1993) contribute in a complex manner to the model–data comparison in the present study.

Vegetation feedback is also very important for climate modelling. Previously, active feedback on the MH SAT north of 50°N and slightly increasing precipitation in the fully coupled ocean–atmosphere–vegetation models (OAVGCMs) compared to OAGCMs were shown by Braconnot et al. (2007b). This finding raises a question regarding vegetation feedback in the East Asian monsoon area and whether the simulated summer precipitation improved in the central parts of China. In future works, we will investigate the vegetation feedback in East Asia using OAVGCMs' simulations within the PMIP2. Moreover, the MH winter climate features will be studied using OAGCMs' and OAVGCMs' simulations as well.

Acknowledgements

This research was supported by the National Basic Research Program (Grant No. 2009CB421406), the Chinese Academy of Sciences (Grant Nos. KZCX2-YW-Q1-02 and KZCX2-YW-Q11-05), and the National Natural Science Foundation of China (Grant Nos. 40631005 and 40775052). We acknowledge the international modelling groups for providing their data for analysis, the Laboratoire des Sciences du Climat et de l'Environnement (LSCE) for collecting and archiving the model data. The PMIP2/MOTIF Data Archive is supported by CEA, CNRS, the EU project MOTIF (EVK2-CT-2002-00153) and the Programme National d'Etude de la Dynamique du Climat (PNEDC). The analyses were performed using version 20-04-2009 of the database. More information is available on <http://pmip2.lsce.ipsl.fr/> and <http://motif.lsce.ipsl.fr/>.

References

An, Z.S., Wu, X.H., Lu, Y.C., Zhang, D.E., Sun, X.J., Dong, G.R., 1990. A preliminary study of the paleoenvironment change of China during the last 20,000 years. In: Liu, T.S. (Ed.), *Loess, Quaternary Geology and Global Change 2*. Beijing, Chinese Science Press, pp. 1–26 (in Chinese).

An, Z.S., Wu, X.H., Wang, P.X., Wang, S.M., Dong, G.R., Sun, X.J., Zhang, D.E., Lu, Y.C., Zheng, S.H., Zhao, S.L., 1991. Paleo-monsoons of China over the last 130,000 years. *Science in China Series B* 14, 1016–1029.

An, C.B., Feng, Z.D., Tang, L.Y., 2003. Evidence of a humid mid-Holocene in the western part of Chinese Loess Plateau. *Chinese Science Bulletin* 48, 2472–2479.

Berger, A.L., 1978. Long-term variations of daily insolation and quaternary climatic changes. *Journal of Atmospheric Sciences* 35, 2362–2367.

Bonfils, C., de Noblet, N., Guiot, J., Bartlein, P., 2004. Some mechanisms of mid-Holocene climate change in Europe, inferred from comparing PMIP models to data. *Climate Dynamics* 23, 79–98.

Braconnot, P., Frankignoul, C., 1993. Testing model simulations of the thermocline depth variability in the tropical Atlantic from 1982 through 1984. *Journal of Physical Oceanography* 23, 626–647.

Braconnot, P., Joussaume, S., Marti, O., de Noblet, N., 1999. Synergistic feedbacks from ocean and vegetation on the African monsoon response to mid-Holocene insolation. *Geophysical Research Letters* 26, 2481–2484.

Braconnot, P., Marti, O., Joussaume, S., Leclainche, Y., 2000. Ocean feedback in response to 6 kyr BP insolation. *Journal of Climate* 13, 1537–1553.

Braconnot, P., Loutre, M.F., Dong, B., Joussaume, S., Valdes, P., PMIP participating groups, 2002. How the simulated change in monsoon at 6 ka BP is related to the simulation of the modern climate: results from the Paleoclimate Modeling Intercomparison Project. *Climate Dynamics* 19, 107–121.

Braconnot, P., Joussaume, S., Harrison, S., Hewitt, C., Valdes, P., Ramstein, G., Stouffer, R.J., Otto-Bliesner, B., Taylor, K.E., 2003. The second phase of the Paleoclimate Modeling Intercomparison Project (PMIP II). *Climate Dynamics* 8, 19–20.

Braconnot, P., Otto-Bliesner, B., Harrison, S., Joussaume, S., Peterchmitt, J.Y., Abe-Ouchi, A., Crucifix, M., Driesschaert, E., Fichefet, Th., Hewitt, C.D., Kageyama, M., Kitoh, A., Laine, A., Loutre, M.F., Marti, O., Merkel, U., Ramstein, G., Valdes, P., Weber, S.L., Yu, Y., Zhao, Y., 2007a. Results of PMIP2 coupled simulations of the mid-Holocene and Last Glacial Maximum – Part 1: experiments and large-scale features. *Climate of the Past* 3, 261–277.

Braconnot, P., Otto-Bliesner, B., Harrison, S., Joussaume, S., Peterchmitt, J.Y., Abe-Ouchi, A., Crucifix, M., Driesschaert, E., Fichefet, Th., Hewitt, C.D., Kageyama, M., Kitoh, A., Loutre, M.F., Marti, O., Merkel, U., Ramstein, G., Valdes, P., Weber, S.L., Yu, Y., 2007b. Results of PMIP2 coupled simulations of the mid-Holocene and Last Glacial Maximum – Part 2: feedbacks with emphasis on the location of the ITCZ and mid- and high latitudes heat budget. *Climate of the Past* 3, 279–296.

Brewer, S., Guiot, J., Torre, F., 2007. Mid-Holocene climate change in Europe: a data-model comparison. *Climate of the Past* 3, 499–512.

Chen, F.H., Shi, Q., Wang, J.M., 1999. Environmental changes documented by sedimentation of Lake Yiema in arid China since the Late Glaciation. *Journal of Paleolimnology* 22, 159–169.

Chen, X., Yu, G., Liu, J., 2002. The climatic simulations and discussion of temperature changes of mid-Holocene over East Asian. *Science in China Series D* 32, 335–345 (in Chinese).

Chen, F.H., Wu, W., Holmes, J.A., Madsen, D.B., Zhu, Y., Jin, M., Oviatt, C.G., 2003a. A mid-Holocene drought interval as evidenced by lake desiccation in the Alashan Plateau, Inner Mongolia, China. *Chinese Science Bulletin* 48, 1401–1410.

Chen, C.T.A., Lan, H.C., Lou, J.Y., Chen, Y.C., 2003b. The dry Holocene megathermal in Inner Mongolia. *Palaeogeography, Palaeoclimatology, Palaeoecology* 193, 181–200.

Christensen, J.H., Hewitson, B., Busuioc, A., Chen, A., Gao, X., Held, I., Jones, R., Kolli, R.K., Kwon, W.-T., Laprise, R., Magaña Rueda, V., Mearns, L., Menéndez, C.G., Räisänen, J., Rinke, A., Sarr, A., Whetton, P., 2007. Regional climate projections. In: Solomon, S., Qin, D., Manning, M., Chen, Z., Marquis, M., Averyt, K.B., Tignor, M., Miller, H.L. (Eds.), *Climate Change 2007: the Physical Science Basis*. Contribution of Working Group I to the Fourth Assessment Report of the Intergovernmental Panel on Climate Change. Cambridge University Press, Cambridge, United Kingdom.

Coe, M.T., Harrison, S.P., 2002. The water balance of northern Africa during the mid-Holocene: an evaluation of the 6 ka BP PMIP simulations. *Climate Dynamics* 19, 155–166.

Crucifix, M., Braconnot, P., Harrison, S.P., Otto-Bliesner, B., 2005. Second phase of Paleoclimate Modelling Intercomparison Project. EOS, *Transactions American Geophysical Union* 86 (28). doi:10.1029/2005EO280003.

Folland, C.K., Rayner, N.A., Brown, S.J., Smith, T.M., Shen, S.S.P., Parker, D.E., Macadam, I., Jones, P.D., Jones, R.N., Nicholls, N., Sexton, D.M.H., 2001. Global temperature change and its uncertainties since 1861. *Geophysical Research Letters* 28, 2621–2624.

Fu, C.B., An, Z.S., Wu, X.D., Wang, M.X., 1992. Past climate changes over China. In: Ye, D.Z., Chen, B.Q. (Eds.), *Global Change Researches in China*. Beijing, China Earthquake Press, pp. 3–82 (in Chinese).

Gasse, F., Arnold, M., Fontes, J.C., Fort, M., Gibert, E., Huc, A., Li, B.Y., Li, Y.F., Liu, Q., Melieres, F., Van Campo, E., Wang, F.B., Zhang, Q.S., 1991. A 13,000-year climate record from western Tibet. *Nature* 353, 742–745.

Gladstone, R.M., Ross, I., Valdes, P.J., Abe-Ouchi, A., Braconnot, P., Brewer, S., Kageyama, M., Kitoh, A., Legrande, A., Marti, O., Ohgaito, R., Otto-Bliesner, B., Peltier, W.R., Vettoretti, G., 2005. Mid-Holocene NAO: a PMIP2 model intercomparison. *Geophysical Research Letters* 32, L16707. doi:10.1029/2005GL023596.

Gordon, C., Cooper, C., Senior, C.A., Banks, H., Gregory, J.M., Johns, T.C., Mitchell, J.F.B., Wood, R.A., 2000. The simulation of SST, sea ice extents and ocean heat transports in a version of the Hadley Centre coupled model without flux adjustments. *Climate Dynamics* 16, 147–168.

Guo, L.L., Feng, Z.D., Li, X.Q., Liu, L.Y., Wang, L.X., 2007. Holocene climatic and environmental changes recorded in Baahar Nuur Lake core in the Ordos Plateau, Inner Mongolia of China. *Chinese Science Bulletin* 52, 959–966.

Harrison, S.P., Jolly, D., Laarif, F., Abe-Ouchi, A., Dong, B., Herterich, K., Hewitt, C., Joussaume, S., Kutzbach, J.E., Mitchell, J., de Noblet, N., Valdes, P., 1998.

- Intercomparison of simulated global vegetation distributions in response to 6 kyr BP orbital forcing. *Journal of Climate* 11, 2721–2742.
- Harrison, S., Braconnot, P., Hewitt, C., Stouffer, R.J., 2002. Fourth international workshop of the Paleoclimate Modelling Intercomparison Project (PMIP): launching PMIP Phase II. *EOS* 83, 447.
- Jacob, R., Schafer, C., Foster, I., Tobis, M., Andersen, J., 2001. Computational design and performance of the fast ocean atmosphere model: version 1. In: Alexandrov, V.N., et al. (Eds.), *The 2001 International Conference on Computational Science*. Springer-Verlag, Berlin, pp. 175–184.
- Jansen, E., Overpeck, J., Briffa, K.R., Duplessy, J.-C., Joos, F., Masson-Delmotte, V., Olago, D., Otto-Bliesner, B., Peltier, W.R., Rahmstorf, S., Ramesh, R., Raynaud, D., Rind, D., Solomina, O., Villalba, R., Zhang, D., 2007. *Palaeoclimate*. In: Solomon, S., Qin, D., Manning, M., Chen, Z., Marquis, M., Averyt, K.B., Tignor, M., Miller, H.L. (Eds.), *Climate Change 2007: The Physical Science Basis. Contribution of Working Group I to the Fourth Assessment Report of the Intergovernmental Panel on Climate Change*. Cambridge University Press, Cambridge, United Kingdom.
- Jiang, W.Y., Liu, T.S., 2007. Timing and spatial distribution of mid-Holocene drying over northern China: response to a southeastward retreat of the East Asian Monsoon. *Journal of Geophysical Research* 112, D24111. doi:10.1029/2007JD009050.
- Jiang, D.B., Wang, H.J., Lang, X.M., 2005. Evaluation of East Asian climatology as simulated by seven coupled models. *Advances in Atmospheric Sciences* 22, 479–495.
- Jiang, W.Y., Guo, Z.T., Sun, X.J., Wu, H.B., Chu, G.Q., Yuan, B.Y., Hatte, C., Guiot, J., 2006. Reconstruction of climate and vegetation changes of Lake Bayanchagan (Inner Mongolia): Holocene variability of the East Asian monsoon. *Quaternary Research* 65, 411–420.
- Jiang, Q.F., Shen, J., Liu, X.Q., Zhang, E.L., Xiao, X.Y., 2007. A high-resolution climatic change since Holocene inferred from multi-proxy of lake sediment in westerly area of China. *Chinese Science Bulletin* 52, 1970–1979.
- Joussaume, S., Taylor, K.E., 1995. Status of the Paleoclimate Modeling Intercomparison Project (PMIP). In: Gates, W.L. (Ed.), *Proceedings of the First International AMIP Scientific Conference*. World Meteorological Organization, Geneva, pp. 425–430. WCRP-92, WMO/TD-732.
- Joussaume, S., Taylor, K.E., Braconnot, P., Mitchell, J.F.B., Kutzbach, J.E., Harrison, S.P., Prentice, I.C., Broccoli, A.J., Abe-Ouchi, A., Bartlein, P.J., Bonfils, C., Dong, B., Guiot, J., Herterich, K., Hewitt, C.D., Jolly, D., Kim, J.W., Kislov, A., Kitoh, A., Loutre, M.F., Masson, V., McAvaney, B., McFarlane, N., de Noblet, N., Peltier, W.R., Peterschmitt, J.Y., Pollard, D., Rind, D., Royer, J.F., Schlesinger, M.E., Syktus, J., Thompson, S., Valdes, P., Vettoretti, G., Webb, R.S., Wyputtu, U., 1999. Monsoon changes for 6000 years ago: results of 18 simulations from the Paleoclimate Modeling Intercomparison Project (PMIP). *Geophysical Research Letters* 26, 859–862.
- K-1 model developers, 2004. K-1 coupled model (MIROC) description. K-1 Technical Report 1, Center for Climate System Research. University of Tokyo, p. 34.
- Kalnay, E., Kanamitsu, M., Kistler, R., Collins, W., Deaven, D., Gandin, L., Iredell, M., Saha, S., White, G., Woollen, J., Zhu, Y., Leetmaa, A., Reynolds, R., Chelliah, M., Ebisuzaki, W., Higgins, W., Janowiak, J., Mo, K.C., Roperewski, C., Wang, J., Jenne, R., Joseph, D., 1996. The NCEP/NCAR 40-year reanalysis project. *Bulletin of the American Meteorological Society* 77, 437–472.
- Kong, S.C., Du, N.Q., Shan, F.S., Tong, G.B., Luo, S.J., Fan, S.X., 1990. Vegetational and climate changes in the last 11,000 years in Qinghai Lake. *Marine Geology & Quaternary Geology* 10, 79–96 (in Chinese).
- Kutzbach, J.E., Guetter, P.J., 1986. The influence of changing orbital parameters and surface boundary conditions on climate simulations for the past 18,000 years. *Journal of Atmospheric Sciences* 43, 1726–1759.
- Kutzbach, J.E., Liu, Z., 1997. Response of the African monsoon to orbital forcing and ocean feedbacks in the middle Holocene. *Science* 278, 440–443.
- Liu, X.Q., Shen, J., Wang, S.M., Yang, X.D., Tong, G.B., Zhang, E.L., 2002. A 16000-year pollen record of Qinghai Lake and its paleoclimate and paleoenvironment. *Chinese Science Bulletin* 47, 1931–1936.
- Marti, O., Braconnot, P., Bellier, J., Benschila, R., Bony, S., Brockmann, P., Cadule, P., Caubel, A., Denvil, S., Dufresne, J.L., Fairhead, L., Filiberti, M.A., Foujols, M.A., Fichefet, T., Friedlingstein, P., Gosse, H., Grandpeix, J.Y., Hourdin, F., Krinner, G., Lévy, C., Madec, G., Musat, I., de Noblet, N., Polcher, J., Talandier, C., 2005. The New IPSL Climate System Model: IPSL-CM4, Note du Pôle de Modélisation, vol. 26. ISSN 1288-1619.
- Masson, V., Joussaume, S., 1997. Energetics of the 6000-yr BP atmospheric circulation in boreal summer, from large-scale to monsoon areas: a study with two versions of the LMD AGCM. *Journal of Climate* 10, 2888–2903.
- Masson, V., Cheddadi, R., Braconnot, P., Joussaume, S., Texier, D., PMIP participants, 1999. Mid-Holocene climate in Europe: what can we infer from PMIP model-data comparisons? *Climate Dynamics* 15, 163–182.
- Mitchell, J.F.B., Grahame, N.S., Needham, K.J., 1988. Climate simulations for 9000 years before present: seasonal variations and effect of the Lasurentide Ice Sheet. *Journal of Geophysical Research* 93, 8283–8303.
- Neff, U., Burns, S.J., Mangini, A., Mudelsee, M., Fleitmann, D., Matter, A., 2001. Strong coherence between solar variability and the monsoon in Oman between 9 and 6 kyr ago. *Nature* 411, 290–293.
- Ohgaito, R., Abe-Ouchi, A., 2009. The effect of sea surface temperature bias in the PMIP2 AOGCMs on mid-Holocene Asian monsoon enhancement. *Climate Dynamics*. doi:10.1007/s00382-009-0533-8.
- Otto-Bliesner, B.L., Brady, E.C., Clauzet, G., Tomas, R., Levis, S., Kothavala, Z., 2006. Last Glacial Maximum and Holocene climate in CCSM3. *Journal of Climate* 19, 2526–2544.
- Peyron, O., Jolly, D., Braconnot, P., Bonnefille, R., Guiot, J., Wirmann, D., Chalié, F., 2006. Quantitative reconstructions of annual rainfall in Africa 6000 years ago: model-data comparison. *Journal of Geophysical Research* 111, D24110. doi:10.1029/2006JD007396.
- Phipps, S.J., 2006. The CSIRO Mk3L Climate System Model. Technical Report No. 3, ISBN 1-921197-03-X, Antarctic Climate & Ecosystems Cooperative Research Centre. Hobart, Tasmania, Australia. pp. 236.
- Roeckner, E., Bauml, G., Bonaventura, L., Brokopf, R., Esch, M., Giorgetta, M., Hagemann, S., Kirchner, I., Kornbluh, L., Manzini, E., Rhodin, A., Schlese, U., Schulzweida, U., Tompkins, A., 2003. The Atmospheric General Circulation Model ECHAM5, Part 1: Model Description. Report, vol. 349, p. 144.
- Rudaya, N., Tarasov, P., Dorofeyuk, N., Solovieva, N., Kalugin, I., Andreev, A., Daryin, A., Diekmann, B., Riedel, F., Tserendash, N., Wagner, M., 2009. Holocene environments and climate in the Mongolian Altai reconstructed from the Hoton-Nur pollen and diatom records: a step towards better understanding climate dynamics in Central Asia. *Quaternary Science Reviews* 28, 540–554.
- Schmidt, G.A., Ruedy, R., Hansen, J.E., Aleinov, I., Bell, N., Bauer, M., Bauer, S., Cairns, B., Canuto, V., Cheng, Y., Genio, A.D., Faluvegi, G., Friend, A.D., Hall, T.M., Hu, Y., Kelley, M., Kiang, N.Y., Koch, D., Lacis, A.A., Lerner, J., Lo, K.K., Miller, R.L., Nazarenko, L., Oinas, V., Perlwitz, J., Perlwitz, J., Rind, D., Romanou, A., Russell, G.L., Sato, M., Shindell, D.T., Stone, P.H., Sun, S., Tausnev, N., Thresher, D., Yao, M.S., 2006. Present-day atmospheric simulations using GISS ModelE: comparison to in situ, satellite, and reanalysis data. *Journal of Climate* 19, 153–192.
- Shen, J., Liu, X.Q., Matsumoto, R., Wang, S.M., Yang, X.D., 2005. A high-resolution climatic change since the Late Glacial Age inferred from multi-proxy of sediments in Qinghai Lake. *Science in China Series D* 48, 742–751.
- Shi, P.J., Song, C.Q., 2003. Palynological records of environmental changes in the middle part of Inner Mongolia, China. *Chinese Science Bulletin* 48, 1433–1438.
- Shi, Y.F., Kong, S.C., Wang, S.M., Tang, L.Y., Wang, F.B., Yao, T.D., Zhao, X.T., Zhang, P.Y., Shi, S.H., 1992. The general characteristics of mid-Holocene climate and environment over China. In: Shi, Y.F. (Ed.), *Mid-Holocene Climate and Environment Over China*. China Ocean Press, Beijing, pp. 1–18 (in Chinese).
- Shi, Y.F., Kong, Z.Z., Wang, S.M., Tang, L.Y., Wang, F.B., Yao, T.D., Zhao, X.T., Zhang, P.Y., Shi, S.H., 1993. Mid-Holocene climates and environments in China. *Global and Planetary Change* 7, 219–233.
- Sun, Q.L., Zhou, J., Shen, J., Chen, P., Wu, F., Xie, X.P., 2006. Environmental characteristics of Mid-Holocene recorded by lacustrine sediments from Lake Daihai, north environment sensitive zone, China. *Science in China Series D* 49, 968–981.
- Tang, L.Y., An, C.B., 2007. Pollen records of Holocene vegetation and climate changes in Longzhong Basin of the Chinese Loess Plateau. *Progress in Natural Science* 17, 1445–1456.
- Tang, L.Y., Shen, C.M., Liu, K., Overpeck, J.T., 2000. Changes in South Asian monsoon: new high-resolution paleoclimatic records from Tibet, China. *Chinese Science Bulletin* 45, 87–91.
- Tao, S.Y., Chen, L.X., 1987. A review of recent research on the east Asian monsoon in China. In: Chang, C.P., Krishnamurti, T.N. (Eds.), *Monsoon Meteorology*. Oxford Univ. Press, New York, pp. 60–92.
- Thompson, L.G., Yao, T., Davis, M.E., Henderson, K.A., Mosley-Thompson, E., Lin, P.N., Beer, J., Synal, H.A., Cole-Dai, J., Bolzan, J.F., 1997. Tropical climate instability: the last glacial cycle from a Qinghai-Tibetan ice core. *Science* 276, 1821–1825.
- Trenberth, K.E., Jones, P.D., Ambenje, P., Bojariu, R., Easterling, D., Klein Tank, A., Parker, D., Rahimzadeh, F., Renwick, J.A., Rusticucci, M., Soden, B., Zhai, P., 2007. Observations: surface and atmospheric climate change. In: Solomon, S., Qin, D., Manning, M., Chen, Z., Marquis, M., Averyt, K.B., Tignor, M., Miller, H.L. (Eds.), *Climate Change 2007: the Physical Science Basis. Contribution of Working Group I to the Fourth Assessment Report of the Intergovernmental Panel on Climate Change*. Cambridge University Press, Cambridge, United Kingdom.
- Wang, H.J., 1992. The seasonal climatic simulation of 9000 years before present by using the IAP atmospheric general circulation model. *Advances in Atmospheric Sciences* 9, 451–457.
- Wang, H.J., 1999. Role of vegetation and soil in the Holocene megathermal climate over China. *Journal of Geophysical Research* 104, 9361–9367.
- Wang, H.J., 2000. The seasonal climate and low frequency oscillation in the simulated mid-Holocene megathermal climate. *Advances in Atmospheric Sciences* 17, 445–457.
- Wang, H.J., 2002. The mid-Holocene climate simulated by a grid-point AGCM coupled with a biome model. *Advances in Atmospheric Sciences* 19, 205–218.
- Wang, S.M., Feng, M., 1992. The relationship between environment change and SE monsoon strength, Daihai Lake, Inner Mongolia. *Science in China Series B* 35, 722–734.
- Wang, Y.J., Cheng, H., Edwards, R.L., He, Y.Q., Kong, X.G., An, Z.S., Wu, J.Y., Kelly, M.J., Dykoski, C.A., Li, X.D., 2005. The Holocene Asian monsoon: links to solar changes and north Atlantic climate. *Science* 308, 854–857.
- Wang, S.Y., Lü, H.Y., Liu, J.Q., Negendank, J.F.W., 2007. The early Holocene optimum inferred from a high-resolution pollen record of Huguangyan Maar Lake in southern China. *Chinese Science Bulletin* 52, 2829–2836.
- Wei, J.F., Wang, H.J., 2004. A possible role of solar radiation and ocean in the mid-Holocene East Asian monsoon climate. *Advances in Atmospheric Sciences* 21, 1–12.
- Wohlfahrt, J., Harrison, S.P., Braconnot, P., Hewitt, C.D., Kitoh, A., Mikolajewicz, U., Otto-Bliesner, B.L., Weber, S.L., 2008. Evaluation of coupled ocean-atmosphere simulations of the mid-Holocene using palaeovegetation data from the northern hemisphere extratropics. *Climate Dynamics* 31, 871–890.
- Wu, Y.H., Lücke, A., Wünnemann, B., Li, S.J., Wang, S.M., 2007. Holocene climate change in the Central Tibetan Plateau inferred by lacustrine sediment geochemical records. *Science in China Series D* 50, 1548–1555.
- Wünnemann, B., Chen, F.H., Riedel, F., Zhang, C.J., Mischke, S., Chen, G.J., Demske, D., Ming, J., 2003. Holocene lake deposits of Bosten Lake, southern Xinjiang, China. *Chinese Science Bulletin* 48, 1429–1432.
- Xie, P.P., Arkin, P.A., 1997. Global precipitation: a 17-year monthly analysis based on gauge observations, satellite estimates, and numerical model outputs. *Bulletin of the American Meteorological Society* 78, 2539–2558.

- Xue, J.B., Zhong, W., 2008. Holocene climate change recorded by lacustrine sediments in Barkou Lake and its regional comparison. *Quaternary Sciences* 28, 610–620 (in Chinese).
- Yao, T.D., Xie, Z.C., Wu, X.L., Thompson, L.G., 1991. Climatic change since little Ice Age recorded by Dunde Ice Cap. *Science in China Series B* 34, 760–767.
- Yu, G., Harrison, S.P., 1996. An evaluation of the simulated water balance of Eurasia and northern Africa at 6000 y BP using lake status data. *Climate Dynamics* 12, 723–735.
- Yu, Y.Q., Zhang, X.H., Guo, Y.F., 2004. Global coupled ocean–atmosphere general circulation models in LASG/IAP. *Advances in Atmospheric sciences* 21, 444–455.
- Yukimoto, S., Noda, A., Kitoh, A., Hosaka, M., Yoshimura, H., Uchiyama, T., Shibata, K., Arakawa, O., Kusunoki, S., 2006. Present-day climate and climate sensitivity in the Meteorological Research Institute coupled GCM version 2.3 (MRI-CGCM2.3). *Journal of the Meteorological Society of Japan* 84, 333–363.
- Zhang, H.C., Ma, Y.Z., Wünnemann, B., Pachur, H.J., 2000. A Holocene climatic record from arid northwestern China. *Palaeogeography, Palaeoclimatology, Palaeoecology* 162, 389–401.
- Zhao, Z.C., Ding, Y.H., Li, X.D., Wang, S.W., 1995. Evaluation of CGCM climate simulation in East Asian region. *Journal of Applied Meteorological Science* 6, 9–18 (in Chinese).
- Zhao, Y., Braconnot, P., Marti, O., Harrison, S.P., Hewitt, C., Kitoh, A., Liu, Z., Mikolajewicz, U., Otto-Bliesner, B., Weber, S.L., 2005. A multi-model analysis of the role of the ocean on the African and Indian monsoon during the mid-Holocene. *Climate Dynamics* 25, 777–800.
- Zhao, Y., Braconnot, P., Harrison, S.P., Yiou, P., Marti, O., 2007a. Simulated changes in the relationship between tropical ocean temperatures and the western African monsoon during the mid-Holocene. *Climate Dynamics* 28, 533–551.
- Zhao, P., Zhu, Y., Zhang, R., 2007b. An Asian–Pacific teleconnection in summer tropospheric temperature and associated Asian climate variability. *Climate Dynamics* 29, 293–303.
- Zhu, C., Ma, C.M., Zhang, W.Q., Zheng, C.G., Tang, L.Y., Lu, X.F., Liu, K.X., Chen, H.Z., 2006. Pollen record from Dajiuhu Basin of Shennongjia and environmental changes since 15.753 ka B.P. *Quaternary Sciences* 26, 814–826 (in Chinese).